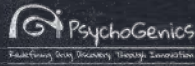


Altered cortical and striatal oscillatory activity in the z_Q175 DN HET knock-in mouse model of Huntington's disease



Sheng Zhong¹, Paul Robichaud¹, Wenjin Xu¹, Afshin Ghavami¹, Vahri Beaumont², Roger Cachepe²

¹PsychoGenics Inc., 215 College Road, Paramus, NJ 07652; ²CHDI Management/CHDI Foundation, 6080 Center Drive, Los Angeles, CA 90045



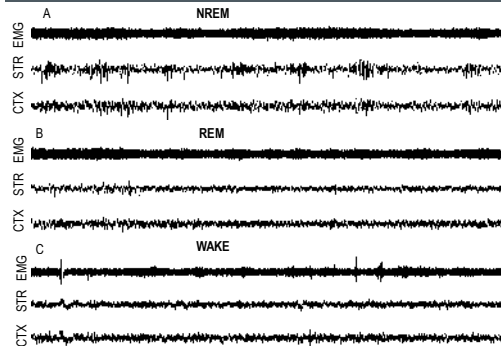
Abstract

Huntington's disease (HD) is a genetically inherited neurodegenerative disorder caused by an expansion of the triplicate CAG repeat in the Huntingtin (HTT) protein. The cortical-striatal loop and MSN neurons in particular are affected in HD^{1,2}. Local field potentials (LFPs), the aggregate electrical activity of a group of neurons, underlie behaviorally relevant neural processing and thus may be useful as a key measurement for understanding the neural basis of the HD behavioral phenotype³. Previous reports have detailed an abnormal increase in gamma oscillations in Q175 het during the wake state in the cortex and striatum⁴. Yet there are no reported deficits in other frequency bands nor an exploration of possible changes in electrocorticogram (ECoG) occurring during different sleep states. In the present study, we replicate findings in the low gamma frequency. In addition, we report a decrease of the delta and theta low frequency bands in cortex as well as striatum and a corresponding increase in the coherence between these brain regions in the z_Q175DN het compared to WT. Furthermore, we observe that these changes are present through both REM and non-REM (NREM) sleep states. Animals were recorded longitudinally from 6-10 months and LFPs in cortex and striatum were separated according to sleep/wake states for analysis.

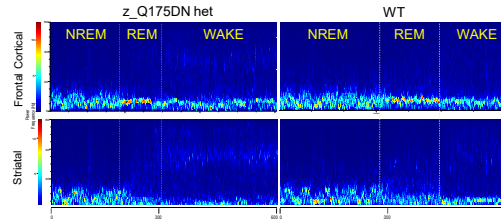
Material and Methods

MANIMALS: z_Q175DN (CHDI-81003019) het (N=12) and WT (N=12) animals were used in the present longitudinal study.
ETHODS: Surgery: Animals were anesthetized with isoflurane (3% for induction and 1-2% for maintenance, at 100% O₂). Five small burr holes were made for the device implant. The ground and common leads were 1.10 screws with wire leads (~3 cm) attached (8403 Prevalve Technology, Inc.). These were screwed into two of the burr holes contra-lateral (ML ±2.0, AP ±2.0 and -4.0mm) to the ECoG recording site. An anchor screw was then screwed into place bilateral and caudal to the ECoG recording lead location (ML ±2.0, AP -4.0mm). All three screws were then secured in place with UV activated acrylic cement (Flow-Bond, LED curing light). The frontal cortex recording lead implant (coated platinum wire 175 μm diameter) was stereotactically lowered in place (AP ±2.0mm, ML ±2.25mm, DV 0.5mm) and secured with UV activated acrylic. The head mount was placed in a stereotaxic holder and the striatal recording lead (attached to the head mount) was then positioned (AP +1.7, ML ±2.0, DV 2.0mm) and secured in place with UV activated acrylic. The common, ground, and frontal cortex lead wires were then soldered to the corresponding locations on the headmount.
ECoG Recordings: ECoGs were recorded continuously using the Pinnacle Technology 8200 data conditioning and acquisition system (DCAS), which performs secondary amplification and filtering before sending data to Pinnacle's Stimsoft Acquisition software for collection via a USB connection (see <http://www.pinnacle.com/3-channel-eeg-systems.html>). ECoG was recorded using 10x gain pre-amplifiers with DCAS amplifier setting at 1000x so the final amplification used in this study is 10,000x with a sampling rate at 1,000 Hz. The signal was filtered by a 500Hz low pass. The pre-amplifier filter was corrected to a low-frequency component mounted above the cage and allows for unencumbered freedom of movement and reduced movement artifacts. Real-time visualization of all ECoG channels from all mice is observed using Stimsoft or PAL-8400 software. One day prior to the recording date, animals were relocated from their home cages to the ECoG recording lab and placed in a circular acrylic mouse cage (cylinder) with 10" diameter, 8" height with water bottle (Pinnacle Technology #8228). The mouse was attached to a cable with preamplifier (#8202; 10x gain), which connects directly to the DCAS head mount via a spin friction fitting on the mouse and to a low-impedance electrical commutator (swivel). Before each session of 24 hours recording, mice were habituated in the recording cage for 1.5 days with the cable connected to head mount. ECoG and striatal oscillatory activity were recorded continuously for 24 hours (start from 12:00 noon to 12:00 noon next day) at 6, 7, 8 and 10 months of age.
History: At the end of the final recording sessions, positions of the recording electrodes for the cortical and striatal recording sites were marked by passing a current (500 mA, 10s) to the recording electrodes to create an identifiable lesion. The brain was then rapidly dissected and frozen on dry ice and transferred to a freezer. Frozen brain sections (20 μm coronal) were cut to verify the recording sites.
Data Analysis: The raw (NREM, REM, Wake) specific frequency bands defined as: 1. Delta 0.5-4 Hz, 2. Theta 4-9 Hz, 3. Alpha 9-12 Hz, 4. Beta 12-30 Hz, 5. Low Gamma 30-60 Hz. Statistics (unpaired t-tests) were run on frequency band data sets only.

Raw Recordings



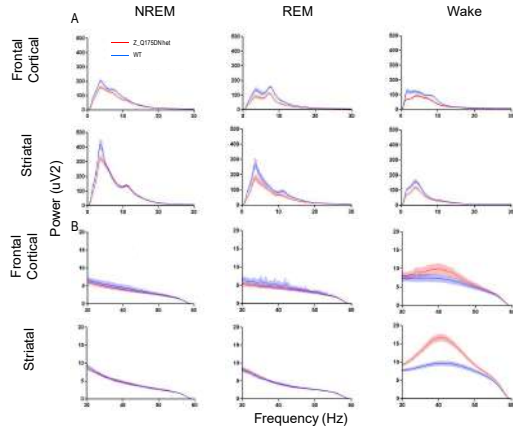
Animal recordings in cortex and striatum were separated by wake and sleep (REM, NREM) states. The above shows representative ECoG traces in the cortex (CTX) and striatum (STR) along with neck electromyogram (EMG) for each state. In the (A) NREM state, ECoG is characterized by increased power in the delta band. In the (B) REM state, ECoG is characterized by increased power in the theta frequency along with a decrease of power in other bands and a flat neck EMG. In the (C) WAKE state, ECoG is not rhythmic and therefore, relatively low power is visualized in the difference frequency bands. This is accompanied by active neck EMG.



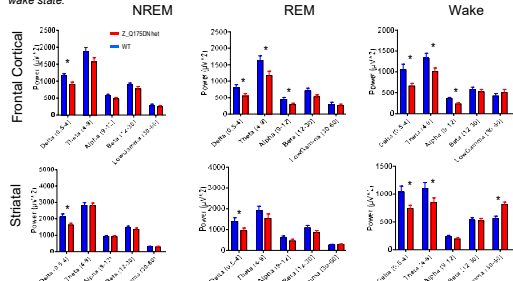
Above are representative spectrograms showing transition between different sleep/wake states in z_Q175DN het and WT animals in both frontal cortex and striatal recordings. Y-axis represents frequency and X-axis is time. Warmer temperatures represent higher power while cooler temperatures demonstrate lower power. Figures show that during REM, z_Q175DN het experience a large increase in power in low frequencies compared to WT in frontal cortex. This difference is less apparent in striatum. In striatal spectrograms, z_Q175DN het show an increase in low gamma power during wake compared to WT.

Results

z_Q175DN HET exhibit altered power in multiple frequency bands compared to WT during sleep and wake states

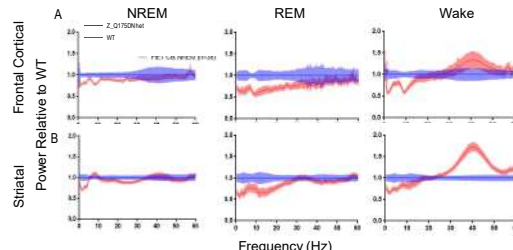


Figures show raw power of 6-10 month old combined recordings in the cortex and striatum of z_Q175DN het compared to WT at all wake states in the (A) 0-30 Hz frequency range and (B) 30-60 Hz frequency range. In the low range, z_Q175DN het demonstrate significantly decreased total power while in the high frequency range, elevations in low gamma is apparent in cortex and striatum during the wake state.



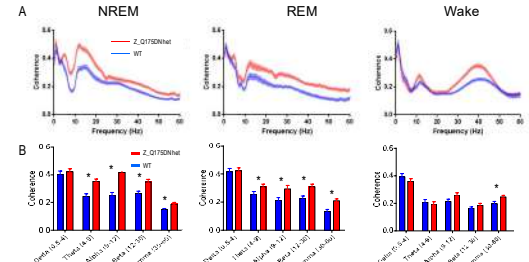
6 to 10 month old data was combined within genotypes. z_Q175DN het mice showed decreased raw power in the delta frequency band at all sleep/wake states as well as in both the cortex ((NREM); t(63), p<0.01, (REM); t(63), p<0.05, (Wake); t(63), p<0.01) and striatum ((NREM); t(63), p<0.01, (REM); t(63), p<0.05, (Wake); t(63), p<0.01). In addition, both cortical theta and alpha frequency ranges were significantly decreased at REM (theta; t(63), p<0.01, alpha; t(63), p<0.01) and wake (theta; t(63), p<0.05, alpha; t(63), p<0.0001) states. In contrast, in dorsolateral striatum, higher frequency ranges appeared to be altered in z_Q175DN het compared to WT. At REM, z_Q175DN het exhibited higher power at high gamma (t(63), p<0.01) while during the wake state, both low t(63), p<0.0001) and high gamma (t(63), p<0.005) frequencies were increased.

Normalized to WT, z_Q175DN HET show differences in LFP power across delta, theta and gamma frequencies at all states



Plots were created by normalizing z_Q175DN het power at different frequency bands to WT measures at the same frequencies. A score of 1 on normalized power suggests z_Q175DN het have the same power compared to WT. A score less than 1 demonstrates lower comparative power and a score higher than 1 demonstrates higher comparative power. Figure illustrates 6-10 month old combined data showing that at both cortex (A) and striatum (B), z_Q175DN het show decreased power compared to WT at delta, theta and alpha frequency bands. At low and high gamma frequency bands, z_Q175DN het show elevated power compared to WT.

Cortical-striatal coherence is increased in z_Q175DN het compared to WT.



Coherence is defined as the coordination of power change between two brain regions. A coherence of 1.0 means that oscillations at a given frequency are perfectly coordinated between two areas. A coherence of 0.0 means that oscillations at a given frequency are not related between two areas. Series A illustrates coherence across frequencies. Series B illustrates binned frequencies. Figures show 6-10 month old combined data for z_Q175DN het and WT. Comparisons via unpaired T-test. During NREM, coherence in the theta (t(63), p<0.0001), alpha (t(63), p<0.0001), beta (t(63), p<0.001) and low (t(63), p<0.01) and high (t(63), p<0.05) gamma frequency bands were significantly elevated in z_Q175DN het compared to WT. The same was true at REM (theta (t(63), p<0.05), alpha (t(63), p<0.05), beta (t(63), p<0.001) and low (t(63), p<0.0001) and high (t(63), p<0.0001) gamma). At wake, only coherence at the gamma frequencies (low (t(63), p<0.05) and high (t(63), p<0.005)) was significantly elevated in z_Q175DN het compared to WT.

State	Genotype	Age	Frequency Bands				
			Delta	Theta	Alpha	Beta	Low Gamma
NREM	Cortex	6M	0.84	0.84	0.84	0.84	0.84
		7M	0.84	0.84	0.84	0.84	0.84
		8M	0.84	0.84	0.84	0.84	0.84
		9M	0.84	0.84	0.84	0.84	0.84
		10M	0.84	0.84	0.84	0.84	0.84
		11M	0.84	0.84	0.84	0.84	0.84
	Striatum	6M	0.84	0.84	0.84	0.84	0.84
		7M	0.84	0.84	0.84	0.84	0.84
		8M	0.84	0.84	0.84	0.84	0.84
		9M	0.84	0.84	0.84	0.84	0.84
		10M	0.84	0.84	0.84	0.84	0.84
		11M	0.84	0.84	0.84	0.84	0.84
REM	Cortex	6M	0.84	0.84	0.84	0.84	0.84
		7M	0.84	0.84	0.84	0.84	0.84
		8M	0.84	0.84	0.84	0.84	0.84
		9M	0.84	0.84	0.84	0.84	0.84
		10M	0.84	0.84	0.84	0.84	0.84
		11M	0.84	0.84	0.84	0.84	0.84
	Striatum	6M	0.84	0.84	0.84	0.84	0.84
		7M	0.84	0.84	0.84	0.84	0.84
		8M	0.84	0.84	0.84	0.84	0.84
		9M	0.84	0.84	0.84	0.84	0.84
		10M	0.84	0.84	0.84	0.84	0.84
		11M	0.84	0.84	0.84	0.84	0.84
WAKE	Cortex	6M	0.84	0.84	0.84	0.84	0.84
		7M	0.84	0.84	0.84	0.84	0.84
		8M	0.84	0.84	0.84	0.84	0.84
		9M	0.84	0.84	0.84	0.84	0.84
		10M	0.84	0.84	0.84	0.84	0.84
		11M	0.84	0.84	0.84	0.84	0.84
	Striatum	6M	0.84	0.84	0.84	0.84	0.84
		7M	0.84	0.84	0.84	0.84	0.84
		8M	0.84	0.84	0.84	0.84	0.84
		9M	0.84	0.84	0.84	0.84	0.84
		10M	0.84	0.84	0.84	0.84	0.84
		11M	0.84	0.84	0.84	0.84	0.84

Tables show unpaired t-test comparisons between WT and z_Q175DN het animals at each age, frequency range and sleep/wake state. Combined age group comparisons are indicated in yellow and significant p-values (0.05) are indicated in blue.

Summary and Conclusions

- In comparison to WT, z_Q175DN het display decreased power in the low frequency ranges in both cortex and striatum, as well as elevated gamma frequency power in striatum.
- z_Q175DN het exhibit higher level of coherence between cortex and striatum across the entire range of the power spectrum during sleep, as compared to WT. During wake, the higher level of coherence is limited to the gamma frequency range.
- Altogether, these results are in line with previous studies characterizing separately cortical and striatal oscillatory activity in rodent models of HD.
- More importantly, the current study provides additional insight on cortico-striatal connectivity in the Q175 mouse model of HD.

- Additional characterization across ages, as well as connectivity among other brain areas might help understand sequentially and potentially causal relationships in HD pathophysiology.

References

- (1993) A novel gene containing a trinucleotide repeat that is expanded and unstable on Huntington's disease chromosomes. The Huntington's Disease Collaborative Research Group. Cell 72:971-983.
- Cepeda C, Wu N, Andre VM, Cummings DM, Levine MS (2007) The corticostriatal pathway in Huntington's disease. Progress in neurobiology 81:253-271
- Fisher SP, Schwartz MD, Wurbs-Black S, Thomas AM, Chen TM, Miller MA, Palmerston JB, Kidduff TS, Meador SR (2016) Quantitative Electroencephalographic Analysis Provides an Early-Stage Indicator of Disease Onset and Progression in the zQ175 Knock-In Mouse Model of Huntington's Disease. Sleep 39:379-391.
- Rothé T, Deliano M, Wojtowicz AM, Dvorzhak A, Harnack D, Poul S, Vagner T, Melnick I, Stark H, Grantin R (2015) Pathological gamma oscillations, impaired dopamine release, synapse loss and reduced.

Acknowledgments and disclosures

CHDI is a private, not for profit biomedical research organization exclusively dedicated to the development of therapies for Huntington's Disease. PsychoGenics is a preclinical Contract Research Organization with expertise in the CNS and orphan disorders.